EXPERIMENTAL REPORT ON EXPERIMENT CH-3606

XAS INVESTIGATION OF CrO_x/SiO_2 CATALYSTS FOR OXIDATIVE DEHYDROGENATION OF PROPANE: THE EFFECT OF DIFFERENT OXIDANTS

EXPERIMENTAL

Cr K-edge EXAFS spectra were collected at the BM23 beamline at the European Synchrotron Radiation Facility (ESRF, Grenoble, F). The white beam was monochromatized using a Si(111) double crystal; harmonic rejection was performed by using silicon mirrors. Due to Cr dilution, EXAFS spectra were collected in fluorescence mode, by means of a Vortex detector (except for the reference Cr_2O_3, measured in transmission). The intensity of the incident beam was monitored by an ionization chamber. The beam transmitted through the sample passed further through a second ionization chamber, a Cr foil and a third ionization chamber to ensure the correct energy calibration for any acquisition.

The samples were measured in the form of pressed pellets inside the cryostat available on BM23, which is small enough to enter in the glove-box. Pellets of samples treated (ex-situ) in different conditions were performed directly inside an argon-filled glove-box and transferred in the cryostat. Measurements were performed at liquid He temperature and in dynamic vacuum (pressure lower than 1.0 10^{-6} Torr) in order to avoid contamination of the samples.

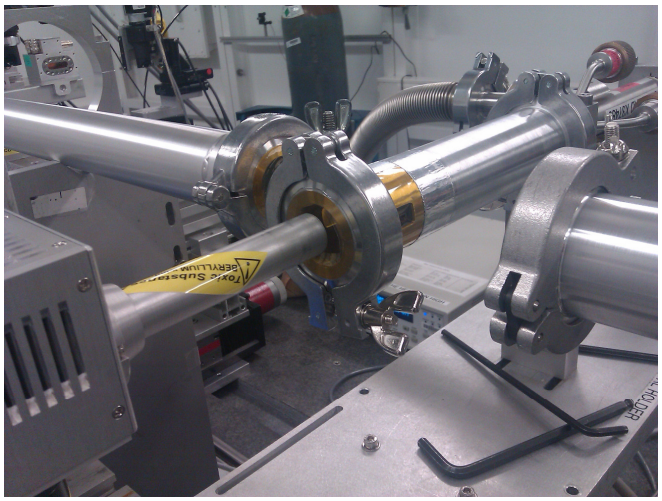

Figure 1 – Picture of the experimental set-up adopted during the measurements of Cr-DHS samples.

The XANES part of the spectra was acquired with an energy step of 0.4 eV and an integration time of 2s/point. The EXAFS part of the spectra was collected up to 15 $Å^{-1}$ with a variable sampling step in energy, resulting in Δk = 0.05 $Å^{-1}$, and an integration time that linearly increases as a function of k from 5 to 20 s/point to account for the low signal-to-noise ratio at high k values. For each sample, six equivalent EXAFS spectra were acquired and averaged before the data analysis.

The extraction of the χ(k) functions was performed using Athena program. Once extracted, the k^3-weighted χ(k) functions were Fourier transformed in a variable Δk range (Δk = 1.0 – 13.0 $Å^{-1}$ range for samples after catalysis, and Δk = 1.0 – 11.0 $Å^{-1}$ for oxidized and reduced samples). The fits were performed in R-space in a variable ΔR range, using the Arthemis program. Phase and amplitudes were calculated by FEFF6.0 code, using as input the structure of Cr_2O_3.

OXIDIZED AND CO-REDUCED CR-DHS SAMPLES

XANES DATA

Figure 2 shows the XANES spectrum of 0.5Cr-DHS sample oxidized at 600°C (black spectrum). The spectrum is very similar to those reported in literature for Cr(VI)/SiO_2 samples having the same chromium loading, employed for both ethylene polymerization (Phillips catalyst)[1-6] and propane ODH reactions. In particular, the intense pre-edge peak centered at 5994 eV (having a shoulder at lower energy values), is characteristic of Cr(VI) species in a T_d-like symmetry. The edge value, evaluated at the maximum of the derivative curve, is at 6007 eV (see Figure 2b).

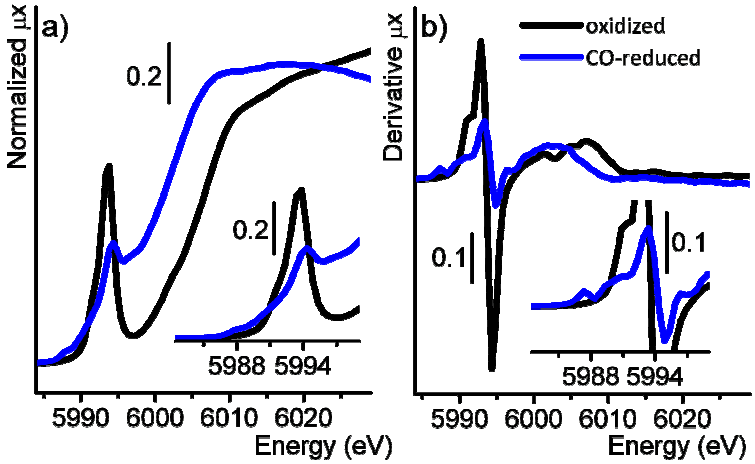

Figure 2 – Normalized XANES spectra (part a) and corresponding derivative signals (part b) of the 0.5Cr-DHS catalyst oxidized (black) and CO-reduced (blue). The two insets show a magnification of the pre-edge region.

The same sample was successively treated in CO at 350°C, following the same procedure usually adopted for the Phillips catalyst,[7] for which it is well known that Cr(VI) sites are selectively converted into Cr(II) species characterized by a high number of coordination vacancies. The spectrum of 0.5Cr-DHS sample treated in CO at 350°C (blue spectrum in Figure 2) is very similar to that reported in literature for an analogous Cr(II)/SiO_2 Phillips catalyst.[8] In particular:

i) the edge is downward shifted (6002 eV) with respect to the oxidized sample, testifying that the treatment in CO caused a reduction of the Cr(VI) sites;

ii) an intense and well resolved pre-edge peak is observed at 5994.2 eV, previously assigned to a Cr1s → Cr4p transition, and considered the fingerprint of isolated Cr(II) sites.[8] It is interesting to observe that this peak is even more resolved than that reported for analogous Cr(II)/SiO_2-aerosil samples, suggesting that the supported Cr(II)

sites in 0.5Cr-DHS samples are more homogeneous; the difference might be due to the different silica support, or to the different synthesis procedure (one-pot vs. wet impregnation), or to both.

iii) additionally, two weak pre-edge features are observed at 5988 and 5990 eV: the same peaks were previously reported for Cr(II)/SiO_2 Phillips catalyst and assigned to Cr1s → (Cr3d + O2p) dipole-forbidden transitions.[8]

In the following, we will consider the XANES spectrum of the 0.5Cr-DHS sample treated in CO at 350°C as representative of well defined (highly uncoordinated) Cr(II) sites.

QUALITATIVE ANALYSIS OF THE ROUGH EXAFS DATA

Figure 3 shows the k^3-weighted χ(k) functions of the 0.5Cr-DHS sample oxidized at 600°C (black) and successively treated in CO at 350°C (blue). The two spectra differ both in the frequency of oscillation and in the total intensity, demonstrating that the local structure around the chromium sites is completely different.

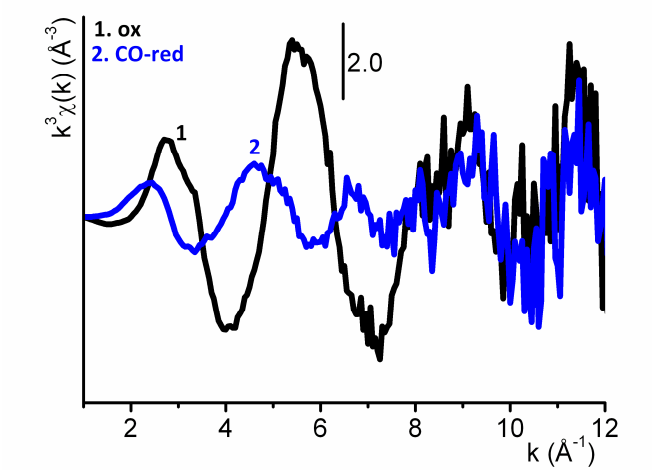

Figure 3 – k^3-weighted χ(k) functions of the 0.5Cr-DHS catalyst oxidized (black) and CO-reduced (blue).

Figure 4 shows the Fourier Transforms of the k^3-weighted χ(k) functions displayed in Figure 3, performed in the Δk = 1.0 – 11.0 Å^{-1} region. As already observed for the rough k^3-weighted χ(k) functions, the two spectra are very different each others. The spectrum of oxidized sample is dominated by an intense signal centered around 1.1 Å (not corrected in phase), having a shoulder around 1.1 Å. The spectrum shows only very weak signals at longer distance, providing an evidence that the Cr sites are essentially isolated. As a matter of fact, the presence of vicinal Cr sites (such as for dichromate structures) would result in a much more intense signal, since chromium is a heavy scatterer ligand compared to oxygen and silicon atoms.

On the contrary, the spectrum of the CO-reduced sample is characterized by a less intense first shell signal at longer distance (1.3 Å), whose intensity is comparable with that of the signal at longer distance (around 2.3 Å). It must be noticed that the low intensity of the spectrum of CO-reduced sample cannot be explained only in terms of a small coordination number; probably, the signals of first shell ligands characterized by a slightly different distance interfere each others in a partially destructive way (as it will be demonstrated in the following).

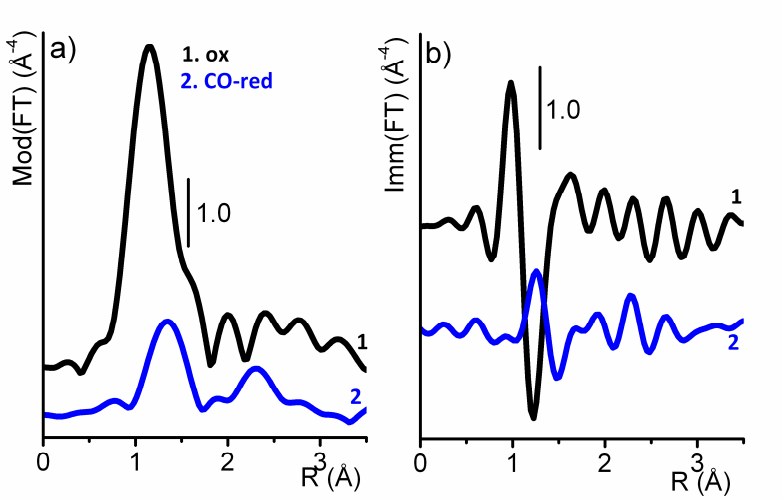

Figure 4 – Fourier Transforms in both modulus (part a) and imaginary parts (part b) of the k^3-weighted χ(k) functions (FT in the Δk = 1.0 – 11.0 Å^{-1} range) of the 0.5Cr-DHS catalyst oxidized (black) and CO-reduced (blue).

EXAFS DATA ANALYSIS

The EXAFS spectrum of the oxidized 0.5Cr-DHS sample was analyzed using as input structure the model shown in Figure 5a, where the absorbing chromium site is in the form of a monochromate, characterized by 2 double-bonded oxygen ligands and grafted to the silica surface through two single-bonded Cr-O ligands.

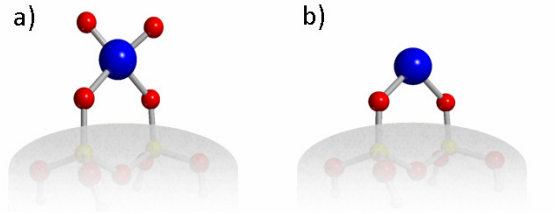

Figure 5 – Schematic representation of surface chromates (part a) and Cr(II) sites (part b) anchored at the silica surface. Hydrogen, oxygen, silicon, and chromium atoms are represented in light grey, red, yellow and blue, respectively.

A first shell analysis was performed by optimizing the following parameters:

i) a single ΔE_0 common to all the paths;
ii) a single S_0^2 value; the coordination numbers for both ligands ($N_{Cr=O}$ and N_{Cr-O}) were both fixed to 2;
iii) the two Cr-O distances ($d_{Cr=O}$ and d_{Cr-O}, respectively).
iv) two Debye-Waller factors for the two ligands ($\sigma^2_{Cr=O}$ and σ^2_{Cr-O}, respectively).

The quality of the fit can be appreciated in Figure 6, where the contributions of the two oxygen ligands is also shown; a summary of the fit results is given in Table 1.

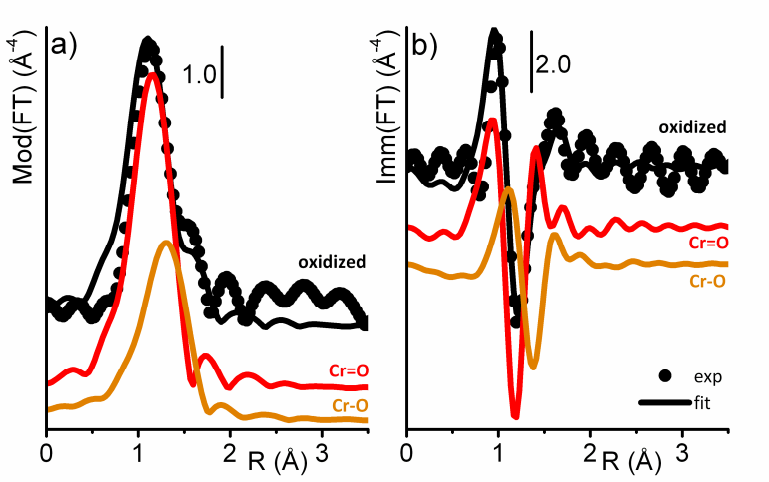

Figure 6 – Phase-uncorrected Fourier Transform (FT) of the $k^3\chi(k)$ EXAFS function for the oxidized 0.5Cr-DHS sample, in both modulus and imaginary parts (parts a and b, respectively); the experimental datum (circles) is overlapped to the best fit (full line). Also the two scattering paths that contribute to the first-shell experimental signal are reported (vertically translated for clarity).

Table 1 – Optimized parameters in EXAFS analysis (performed in the ΔR = 1.0 – 3.0 Å range, FT in 1.0–11.0 A^{-1} k-range) for the oxidized 0.5Cr-DHS catalyst. The coordination numbers were kept fixed, and a single S_0^2 value was fitted. The fit resulted in R_{factor}= 0.08.

ligand	ΔE (eV)	S_0^2	N	R (Å)	σ^2 (Å^2)
O (Cr=O)	3 ± 5	0.8 ± 0.2	2	1.60 ± 0.03	0.004 ± 0.003
O (Cr-O)			2	1.78 ± 0.04	0.006 ± 0.005

The fit confirms that the model shown in Figure 5a represents well the local structure of the chromium sites in oxidized 0.5Cr-DHS sample: in average, the chromium sites are in the form of monochromates, with 2 oxygen ligands at 1.60 Å (double-bonded) and 2 oxygen ligands at 1.78 Å (single-bonded). It is interesting to observe that the DW factors are quite small for both ligands (indicative of a quite homogeneous situation), but smaller for the Cr=O contribution, as expected because the double-bond is stronger than the single-one. Similar results were previously reported in literature for other Cr(VI)/SiO_2 samples.[1, 5, 7, 9]

The analysis of the spectrum for the CO-reduced 0.5Cr-DHS sample was less straightforward. As a matter of fact, the very small amplitude of the EXAFS oscillations in the k^3-weighted χ(k) functions (see Figure 3) implies a low accuracy in the determination of the coordination numbers. It was not possible to fit the datum by leaving free all the fitting variables. Therefore, the fit was performed by fixing S_0^2 to the value found for the oxidized sample. The best fit was obtained by considering, in addition to the ligands shown in Figure 5b, also one O ligand at a slightly longer distance. The quality of the fit can be appreciated in Table 4, where the contributions of the relevant paths is also shown; a summary of the fit results is given in Table 2.

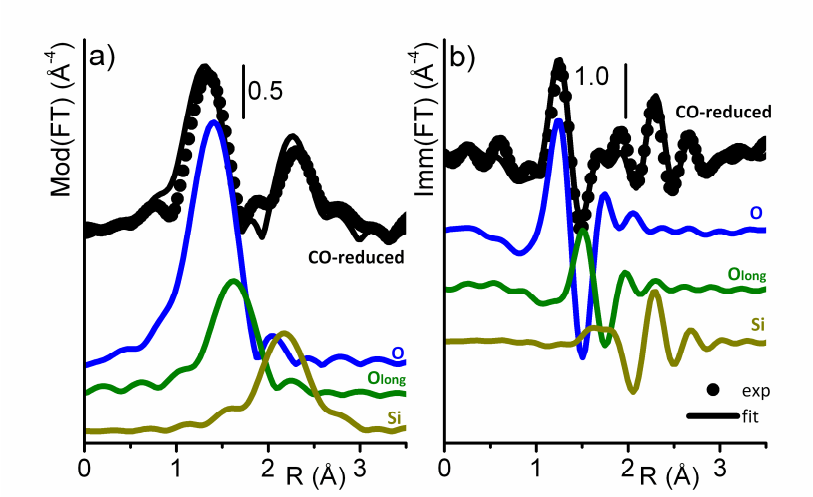

Figure 7 – Phase-uncorrected Fourier Transform (FT) of the $k^3\chi(k)$ EXAFS function for the CO-reduced 0.5Cr-DHS sample, in both modulus and imaginary parts (parts a and b, respectively); the experimental datum (circles) is overlapped to the best fit (full line). Also the three scattering paths that mainly contribute to the experimental signal are reported (vertically translated for clarity).

Table 2 – Optimized parameters in EXAFS analysis (performed in the ΔR = 1.0 – 3.0 Å range, FT in 1.0–11.0 A^{-1} k-range) for the CO-reduced 0.5Cr-DHS catalyst. The coordination numbers were kept fixed, and the S_0^2 value was fixed to that found for the oxidized sample. The fit resulted in R_{factor}= 0.09.

ligand	ΔE (eV)	S_0^2	N	R (Å)	σ^2 (Å^2)
O short	0 ± 3	0.8	2	1.90 ± 0.02	0.010 ± 0.002
O long			1	2.13 ± 0.04	0.006 ± 0.004
Si			2	2.71 ± 0.03	0.008 ± 0.003

The fit results are in good agreement with those previously reported by some of us for a similar Cr(II)/SiO_2 sample.[8] In average, each chromium site is surrounded by 2 oxygen ligands at a distance of 1.90 ± 0.02 Å (previous results: 2 O ligands at 1.86 ± 0.03 Å), and by 2 silicon ligands at 2.71 ± 0.03 Å (previous results: 2 Si ligands at 2.70 ± 0.02 Å). In addition, 1 oxygen ligand at 2.13 ± 0.04 Å is necessary to fit the data, whereas about 3 additional oxygen ligands at a longer distance (2.64 ± 0.03 Å) were found in our previous work.[8] The oxygen ligands at longer distance likely belong to surface siloxane bridges weakly bonded to the chromium sites. The smaller number of second-shell oxygen ligands necessary to fit the experimental spectrum of the here analyzed sample might be a consequence of the different type of silica support (MCM vs. aerosil) or of the synthesis method (one pot vs. impregnation), or both. The EXAFS data suggest that Cr(II) sites in Cr-DHS samples are characterized by a greater number of coordination vacancies with respect to those in Cr(II)/SiO_2.

Cr-DHS samples in different Propane ODH reaction conditions

XANES data

Figure 8 shows the normalized XANES spectra (part a) and their derivative signals (part b) of the oxidized 1.0Cr-DHS samples treated in different propane ODH reaction conditions, compared to that of the Cr_2O_3 reference compound. The spectra can be divided in two main groups. When propane ODH reaction is performed without any oxidant, the XANES spectrum shows the edge (evaluated at the maximum of the derivative curve, Figure 8b) at 6002 eV and is characterized by an intense and broad pre-edge peak centered around 5996 eV, and by two weak pre-edge peaks at 5988 and 5990 eV. All these features are indicative of the presence of highly reduced Cr(II) species, as testified by the close similarity of the spectrum with that of CO-reduced sample (blue in Figure 2). The XANES spectrum of the sample reacted in presence of propane and CO_2 (light green) is practically undistinguishable from the one just discussed, as better observed in the derivative signals (Figure 8b).

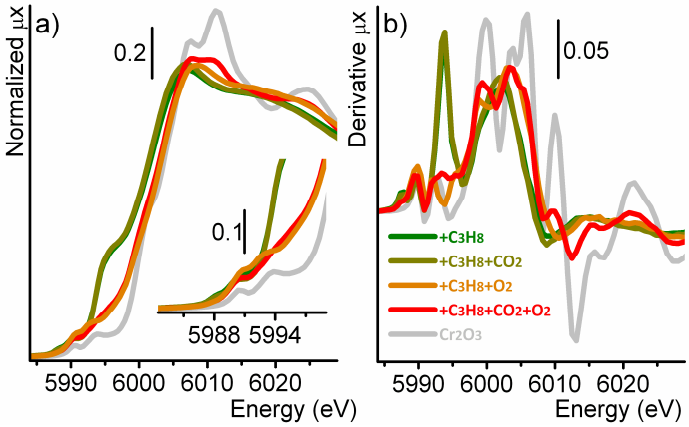

Figure 8 – Normalized XANES spectra (part a) and corresponding derivative signals (part b) of the oxidized 1.0Cr-DHS catalyst treated in different propane ODH reaction conditions: only propane (green), propane + CO_2 (light green), propane +O_2 (red) and propane + CO_2 + O_2 (orange). Also the spectrum of Cr_2O_3 reference is shown for comparison (grey). Inset in part a) shows a magnification of the pre-edge region.

On the contrary, when propane ODH reaction is performed in presence of O_2 (orange) the XANES spectrum shows a double edge at 5999 and 6003 eV (see derivative signal, Figure 8b), very similar to that shown by Cr_2O_3 reference compound. In the pre-edge region two weak pre-edge peaks are observed at 5990 and 5993 eV (the same present in the spectrum of Cr_2O_3), whereas the intense pre-edge peak around 5996 eV characteristic of Cr(II) species is not present; only a shoulder is observed. The spectrum of the sample after propane ODH reaction in presence of the mixture O_2+CO_2 (red) is even more similar to that of Cr_2O_3. In particular, in the white-line region two peaks are observed at 6008 and 6010 eV, which are characteristic of the multiple-scattering contributions of Cr_2O_3-like particles.

In all cases, XANES spectra suggest that two chromium phases are present in the 1.0Cr-DHS samples after the catalysis: i) a Cr_2O_3-like phase, where the chromium sites have a +3 oxidation state and display a pseudo-octahedral coordination; and ii) a Cr(II) containing phase, where the chromium sites are highly uncoordinated as for isolated Cr(II) sites obtained after CO-reduction. In principle, it is possible to quantitatively evaluate the amount of each phase present in the samples by fitting each spectrum with a simple linear

combination of the two reference phases. The results of the fits (performed on the normalized XANES spectra in the ΔE = -20 – 15 eV region, without constraints) are summarized in Table 3.

Table 3 – Quantitative estimation of the relative amount of Cr_2O_3-like and Cr(II)-like phases present in the 1.0Cr-DHS samples treated in different propane ODH reaction conditions, as determined by fitting the XANES spectra with a linear combination of the two reference phases. The fit were performed on the normalized XANES spectra, in the ΔE = -20 – 15 eV region, without any constraint.

phase	**Propane ODH reaction conditions**			
	C_3H_8	$C_3H_8 + CO_2$	$C_3H_8 + O_2$	$C_3H_8 + CO_2 + O_2$
Cr_2O_3 - like	0.41 ± 0.01	0.45 ± 0.01	0.59 ± 0.02	0.64 ± 0.02
CO-reduced like	0.63 ± 0.01	0.59 ± 0.02	0.40 ± 0.03	0.38 ± 0.02

The data shown in Table 3 demonstrate that after the catalysis the starting Cr(VI) sites are reduced to a mixture of Cr(III) and Cr(II), whose relative proportion depends on the propane ODH reaction conditions: in presence of C_3H_8 only, or of $C_3H_8 + CO_2$, about 40% of the chromium sites are reduced to Cr(III), whereas the fraction of Cr(III) increases to about 60% when the reaction is performed in presence of O_2 or O_2+CO_2. The fact that the sum of the two fitted fractions is close to 1 without imposing any constraints guarantees the validity of the approach.

QUALITATIVE ANALYSIS OF THE ROUGH EXAFS DATA

The k^3-weighted χ(k) functions of the 1.0Cr-DHS catalyst treated in different propane ODH reaction conditions are shown in Figure 9 and compared to that of Cr_2O_3 (multiplied by 0.65). The spectra of the catalysts are very similar each others and also to that of Cr_2O_3 in terms of average oscillations, although less intense. However, while the first three spectra are characterized by smooth oscillations, the spectrum of the sample treated in presence of all the reagents (propane, O_2 and CO_2) shows the sharp beats characteristic of the spectrum of Cr_2O_3, which are due to the contribution of chromium ligands in the second and third coordination shells at slightly different distance (see discussion in the appendix).

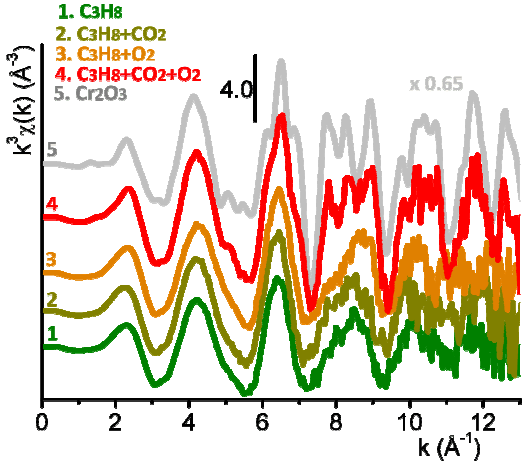

Figure 9 – k^3-weighted χ(k) functions of the oxidized 1.0Cr-DHS catalyst treated in different propane ODH reaction conditions: only propane (green), propane + CO_2 (light green), propane +O_2 (red) and propane + CO_2 + O_2 (orange). Also the spectrum of Cr_2O_3 (grey, multiplied by a factor of 0.65) is shown for comparison.

Figure 10 shows the Fourier Transforms of the k^3-weighted χ(k) functions displayed in Figure 9, performed in the Δk = 1.0 – 13.0 $Å^{-1}$ region. Also the spectrum of Cr_2O_3 (grey, multiplied by a factor of 0.65) is shown for comparison. As already observed for the rough k^3-weighted χ(k) functions, the spectra of the first three samples are very similar each others. They are dominated by a first shell signal centered around 1.5 Å (not corrected in phase), as for Cr_2O_3 although 1/3 less intense; and by a broad signal around 2.6 Å, similar to the second shell signal characteristic of Cr_2O_3, but less intense and shifted at longer distance (well evident in the Imm(FT), Figure 10b). The spectrum of the catalyst treated in presence of all the reagents is more similar to that of Cr_2O_3. In particular, it is worth noticing the presence of a third shell signal around 3.2 Å (absent in the spectra of the other catalysts).

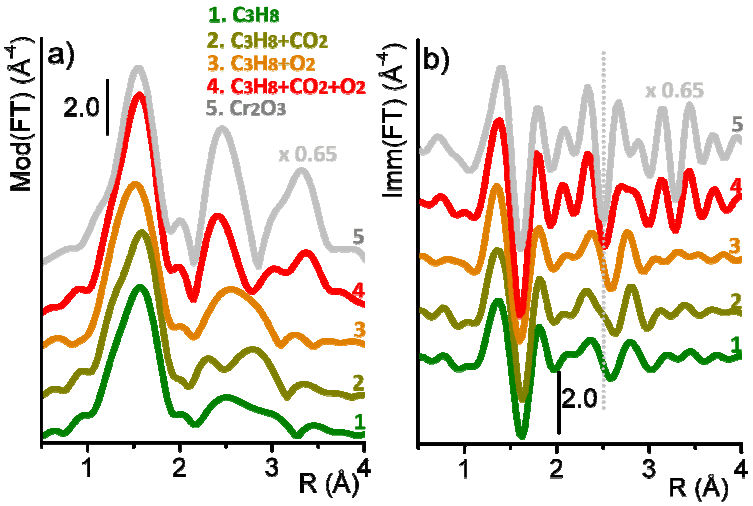

Figure 10 – Fourier Transforms in both modulus (part a) and imaginary parts (part b) of the k^3-weighted χ(k) functions (FT in the Δk = 1.0 – 13 $Å^{-1}$ range) of the oxidized 1.0Cr-DHS catalyst treated in different propane ODH reaction conditions: only propane (green), propane + CO_2 (light green), propane +O_2 (red) and propane + CO_2 + O_2 (orange). Also the spectrum of Cr_2O_3 (grey, multiplied by a factor of 0.65) is shown for comparison.

EXAFS DATA ANALYSIS OF THE 1.0CR-DHS CATALYSTS TREATED IN ODH REACTIONS

In the analysis of the EXAFS data, it is necessary to take into account the fact that XANES data demonstrate the presence of two different phases in all the samples, differing in both the oxidation state and coordination geometry. Therefore, a correct approach should imply a 2-phases analysis, as reported in literature for similar systems.[5] Nevertheless, we have also demonstrated that the EXAFS signal characteristic of the Cr(II)/SiO_2 phase is much less intense than the oscillations of Cr_2O_3-like phase; hence, we expect that the experimental signal of a mixture of Cr(III) and Cr(II)-like phases is dominated by the Cr_2O_3-like phase. For this reason, we performed a preliminary data analysis by considering only the Cr_2O_3-like contribution. In a second moment, we improved the level of calculation by performing a two phase analysis. The two approaches will be discussed separately.

SINGLE PHASE ANALYSIS

In a preliminary attempt, we performed an analysis by considering the presence of a Cr_2O_3-like phase only. For the first 3 catalysts (i.e. treated in presence of propane only, propane +CO_2, and propane + O_2), the analysis was performed by using Cr_2O_3 as input structure and by considering two scattering paths only: a) a Cr-O for the first shell signal and b) a Cr-Cr path for the second shell signal. As a matter of fact, the absence in the Imm(FT) of the beats characteristic of Cr_2O_3 suggests that only one type of chromium ligand contributes to the second shell signal. In all the three cases, the fit was performed by optimizing the following parameters:

i) a single ΔE_0 common to all the paths;
ii) the coordination numbers for both ligands (N_O and N_{Cr}, respectively); the resulting N values were re-normalized to the S_0^2 value obtained by fitting the signal of the Cr_2O_3 reference compound (0.7);
iii) the two Cr-L distance;
iv) two Debye-Waller factors for the two ligands (σ^2_O and σ^2_{Cr}, respectively).

The quality of the fits can be appreciated in Figure 11, Figure 12, and Figure 13, where the two scattering paths that contribute to the experimental signal are also reported. A summary of the fit results are given in Table 4, Table 5, and Table 6.

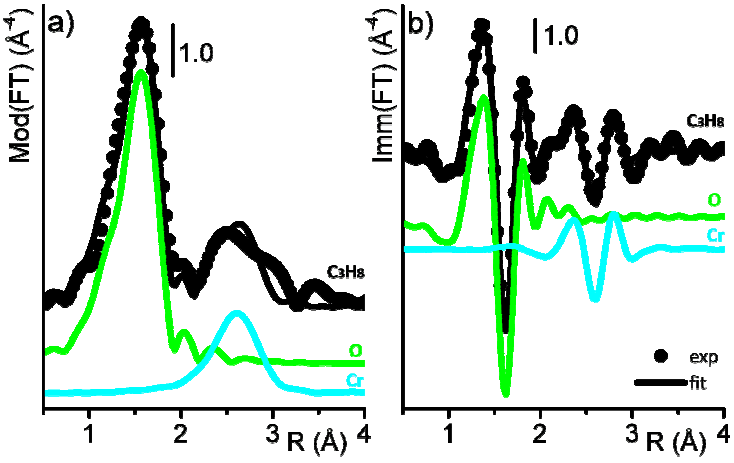

Figure 11 – Phase-uncorrected Fourier Transform (FT) of the $k^3\chi(k)$ EXAFS function for the catalyst treated in C_3H_8, in both modulus and imaginary parts (parts a and b, respectively); the experimental datum (circles) is overlapped to the best fit (full line). Also the two scattering paths that contribute to the experimental signal are reported (vertically translated for clarity).

Table 4 – Optimized parameters in EXAFS analysis (performed in the ΔR = 0.0 – 4.0 Å range, FT in 1.0–13.0 A^{-1} k-range) for the 1.0Cr-DHS catalyst treated in presence of C3H8 only. The coordination numbers have been re-normalized to the S_0^2 value obtained by fitting the signal of the Cr_2O_3 reference compound (S_0^2 = 0.7). The fit resulted in R_{factor}= 0.035.

	ΔE (eV)	**N**	**R (Å)**	**σ^2 (Å^2)**
O	0 ± 1	3.3 ± 0.3	2.009 ± 0.007	0.0057 ± 0.0009
Cr		1.9 ± 0.9	3.04 ± 0.02	0.012 ± 0.004

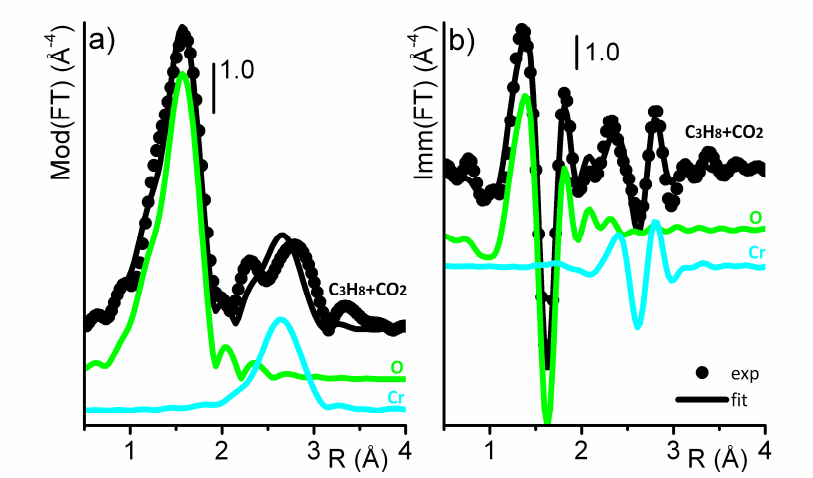

Figure 12 –As for Figure 11, for the catalyst treated in C_3H_8 + CO_2.

Table 5 – As for Table 4 for the 1.0Cr-DHS catalyst treated in presence of C_3H_8 + CO_2. The fit resulted in R_{factor}= 0.039.

	ΔE (eV)	**N**	**R (Å)**	**σ^2 (Å^2)**
O	0 ± 1	3.7 ± 0.3	2.017 ± 0.008	0.0058 ± 0.0009
Cr		1.6 ± 0.6	3.05 ± 0.02	0.009 ± 0.003

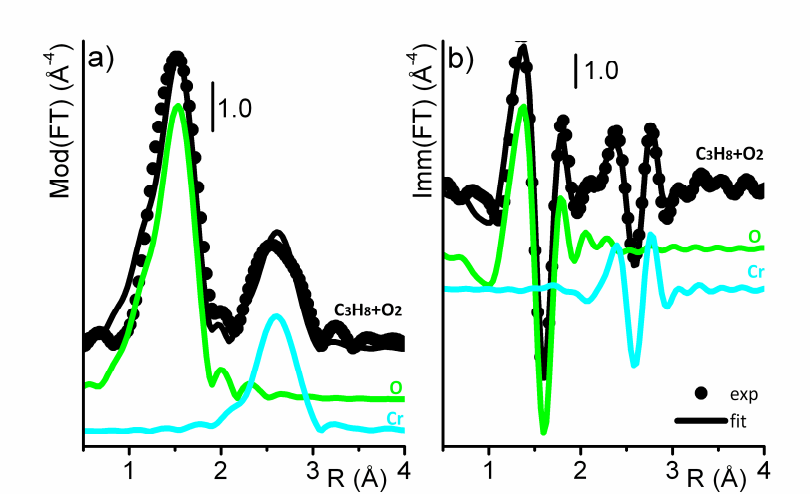

Figure 13 – As for Figure 11, for the catalyst treated in $C_3H_8 + O_2$.

Table 6 – As for Table 4 for the 1.0Cr-DHS catalyst treated in presence of $C_3H_8 + O_2$. The fit resulted in R_{factor}= 0.055.

	ΔE (eV)	**N**	**R (Å)**	**σ^2 (Å^2)**
O	-2 ± 1	3.7 ± 0.4	1.985 ± 0.009	0.006 ± 0.009
Cr		1.5 ± 0.9	3.01 ± 0.02	0.006 ± 0.004

The spectrum of the sample treated in C_3H_8+O_2+CO_2 was analyzed by considering five scattering paths: a) a Cr-O path for the first shell; b) two Cr-Cr paths for the second shell; c) two Cr-Cr paths for the third shell. Indeed, the presence of the beats at about 2.1 Å and 2.9 Å suggests that 2 Cr-Cr paths contribute in the same ΔR region. The results of the fit are summarized in Table 7, and the quality of the fit can be appreciated by looking at Figure 13.

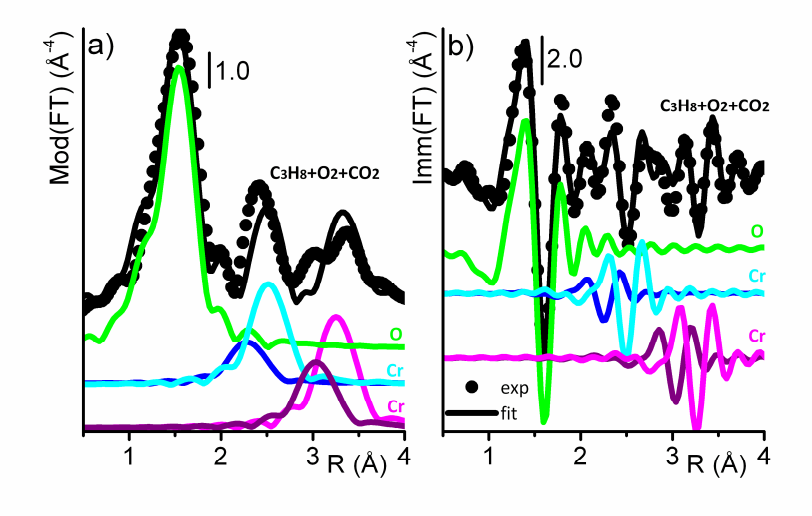

Figure 14 – As for Figure 11, for the catalyst treated in C_3H_8 + O_2 + CO_2.

Table 7 – As for Table 4 for the 1.0Cr-DHS catalyst treated in presence of C_3H_8 + O_2 + CO_2. The fit resulted in R_{factor}= 0.080.

	ΔE (eV)	**N**	**R (Å)**	**σ^2 (Å^2)**
O	-3 ± 1	4.0 ± 0.7	1.98 ± 0.01	0.004 ± 0.001
Cr1		0.4 ± 0.2	2.68 ± 0.01	0.004 ± 0.002
Cr2		1.2 ± 0.2	2.91 ± 0.01	0.004 ± 0.002

In all the cases, although a single chromium phase was used to fit the experimental data instead of the two expected, the quality of the fits is good. In average:

i) the first shell is composed of less than 4 oxygen ligands at an average distance of about 2.0 Å, to be compared with the 6 ligands at 1.995 Å in Cr_2O_3.
ii) The second shell is constituted by less than 2.0 chromium ligands at an average distance of 3.0 Å, to be compared with 3 Cr at 2.90 Å + 1 Cr at 2.66 Å in Cr_2O_3. The Cr-Cr distances are close to those characteristic of Cr_2O_3 for the catalyst treated in presence of all the reagents.

Although the first shell Cr-O distance is very close to that characteristic of Cr_2O_3, the average coordination number is smaller than that expected for O-terminated CrO_6 octahedra. This result is in perfect agreement with the co-presence of a second phase (Cr(II)-like), where chromium sites are less coordinated than in Cr_2O_3, and at a slightly different distance.

TWO PHASES ANALYSIS

In a second moment, we tried to perform a 2-phases analysis, considering the co-presence of a Cr(II)/SiO_2-like phase and of a Cr_2O_3-like phase, having the following properties: i) the Cr(II)/SiO_2-like phase contributes only in the first shell signal with 2 oxygen ligands, being the corresponding signal quite weak; ii) the Cr_2O_3-like phase contributes to the first shell signal with 6 oxygen ligands, and also to the second shell one, with a number of Cr ligands that depends on the dimension of the Cr_2O_3-like particles. The fits were performed by considering 3 scattering paths: a) a Cr-O path for the Cr(II)/SiO_2-like phase, Cr-O_{II}; b) a Cr-O path for the Cr_2O_3-like phase, Cr-O_{III}; c) a Cr-Cr path for the Cr_2O_3-like phase contributing to the second shell signal.

In all the cases, the fit was performed by fitting the following variables:

i) a single ΔE_0 common to all the paths;

ii) the fraction x of the Cr_2O_3-like phase, being defined as (1-x) the fraction of Cr(II)/SiO_2-like phase;

iii) the amplitude of the Cr-Cr contribution, amp_Cr; from amp_Cr the N_{Cr} coordination number characteristic of the second shell around the absorbing sites can be obtained:

iv) the Cr-O_{II}, Cr-O_{III} and Cr-Cr distances;

v) two Debye-Waller factor for the Cr-Cr contribution,σ^2_{Cr}.

The amplitude of the Cr-O_{II} and Cr-O_{III} contributions were defined as:

amp_O_{III} = N(Cr-O_{III}) * S^0_2 * x

amp_O_{II} = N(Cr-O_{II}) * S^0_2 * (1-x)

being N(Cr-O_{III}) = 6, N(Cr-O_{II}) = 2, and S^0_2 = 0.8 (as determined from the analysis of the reference Cr_2O_3). Finally, the Debye-Waller factors for the two Cr-O contributions were fixed to the values found for the two reference phases. This choice was dictated by the strong correlation between σ^2 and coordination numbers N.

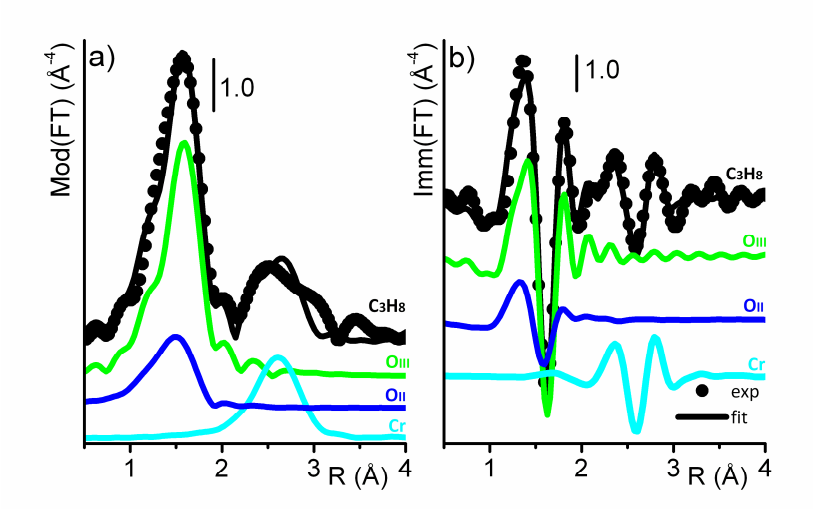

Figure 15 – Phase-uncorrected Fourier Transform (FT) of the $k^3\chi(k)$ EXAFS function for the catalyst treated in C_3H_8, in both modulus and imaginary parts (parts a and b, respectively); the experimental datum (circles) is overlapped to the best fit (full line) performed with a 2-phases analysis. Also the 3 scattering paths that contribute to the experimental signal are reported (vertically translated for clarity).

Table 8 – Optimized parameters in EXAFS analysis (performed in the ΔR = 1.0 – 4.0 Å range, FT in 1.0–13.0 A^{-1} k-range) for the 1.0Cr-DHS catalyst treated in presence of C_3H_8 only. Values without errors have been fixed. The fit resulted in R_{factor}= 0.041.

	x	ΔE (eV)	N	R (Å)	σ^2 (Å^2)
O_{II}	0.38 ± 0.06	0 ± 1	2	1.98 ± 0.06	0.0034
O_{III}			6	2.014 ± 0.009	0.010
Cr			1.9 ± 0.8	3.04 ± 0.02	0.012 ± 0.005

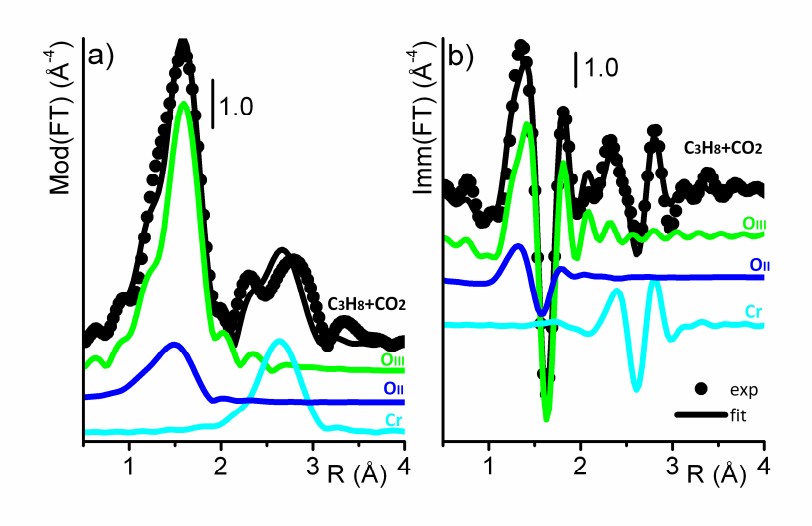

Figure 16 –As for Figure 15, for the catalyst treated in C_3H_8 + CO_2.

Table 9 – As for Table 8 for the 1.0Cr-DHS catalyst treated in presence of C_3H_8 + CO_2. The fit resulted in R_{factor}= 0.044.

	x	ΔE (eV)	N	R (Å)	σ^2 (Å^2)
O_{II}	0.47 ± 0.09	0 ± 2	2	1.97 ± 0.08	0.0034
O_{III}			6	2.021 ± 0.008	0.010
Cr			1.3 ± 0.6	3.05 ± 0.02	0.009 ± 0.004

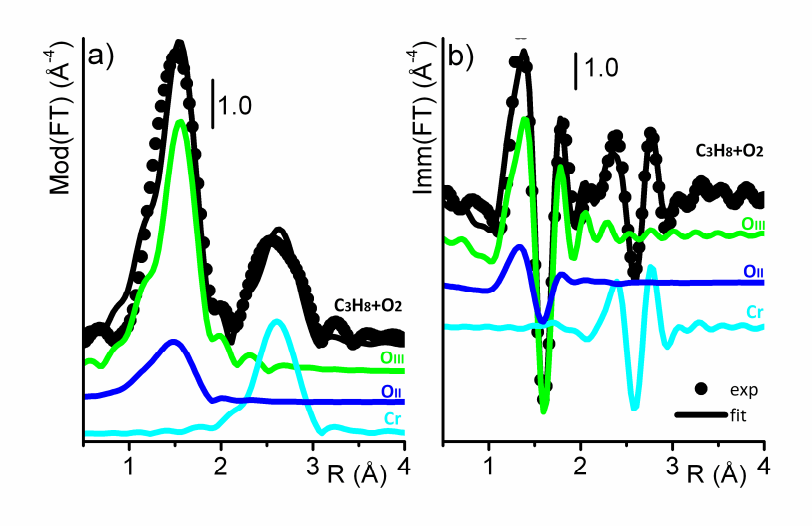

Figure 17 –As for Figure 15, for the catalyst treated in C_3H_8 + O_2.

Table 10 – As for Table 8 for the 1.0Cr-DHS catalyst treated in presence of C_3H_8 + O_2. The fit resulted in R_{factor}= 0.072.

	x	ΔE (eV)	N	R (Å)	σ^2 (Å^2)
O_{II}	0.53 ± 0.07	-1 ± 2	2	1.97 ± 0.09	0.0034
O_{III}			6	2.00 ± 0.02	0.010
Cr			1.3 ± 0.9	3.02 ± 0.02	0.007 ± 0.005

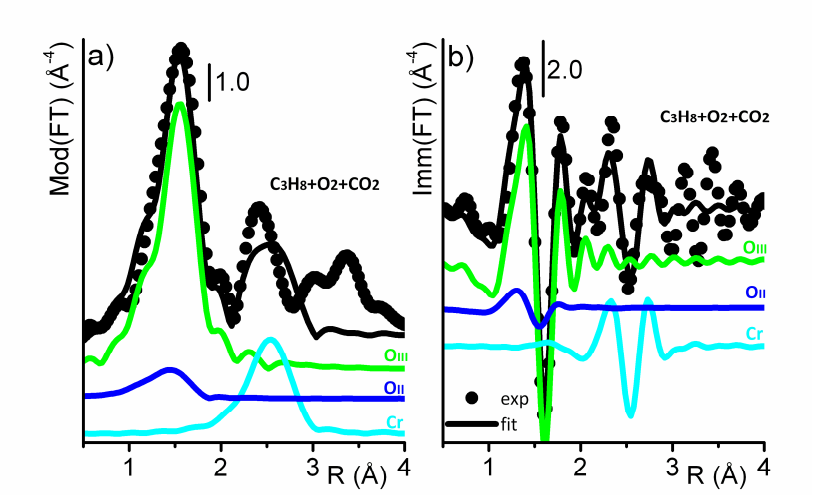

Figure 18 –As for Figure 15, for the catalyst treated in C_3H_8 + O_2 + CO_2.

Table 11 – As for Table 8 for the 1.0Cr-DHS catalyst treated in presence of C_3H_8 + O_2 + CO_2. The fit resulted in R_{factor}= 0.13.

	x	ΔE (eV)	N	R (Å)	σ^2 (Å^2)
O_{II}	0.64 ± 0.2	-2 ± 4	2	1.93 ± 0.3	0.0034
O_{III}			6	2.00 ± 0.02	0.010
Cr			1.4 ± 0.9	2.97 ± 0.03	0.009 ± 0.007

GENERAL DISCUSSION

The results of the 2-phases fits are consistent with those of the single-phase fits, although the quality is slightly worst. This is due to the fact that some variables were fixed, because of correlation problems. Nevertheless, the two-phase analysis allows to draw the following conclusions, common to all the samples:

i) the fraction x of the Cr_2O_3-like phase present in each sample as a function of the reaction conditions is in perfect agreement with the values determined by XANES analysis. Hence, the co-presence of two chromium phases is fully confirmed. Their relative amount was estimated by means of two independent analysis, the former mainly based on the evaluation of the chromium oxidation state and the latter on the structure around the absorbing chromium sites.

ii) The 2-phases analysis allows to explain the first shell N_O coordination numbers obtained in the single-phase analysis, which are smaller than the values of 6 expected for a Cr_2O_3-like phase. This is due to the co-presence of a second phase (Cr(II)/SiO_2-like) where the chromium sites are surrounded by less oxygen ligands at a slightly shorter distance.

iii) The second shell Cr-Cr contribution is characterized by a N_{Cr} coordination number smaller than that expected for a Cr_2O_3-like phase, also when the relative fraction of this phase is considered. This suggests that in the Cr_2O_3-like phase the CrO_6 octahedra are, in average, organized in dimers or trimers.

Taken all together, these data (and the XANES spectra discussed above) suggest that during the catalysis two chromium phases coexist, whose relative proportion depends on the reaction environment: i) a Cr(II)/SiO_2-like phase, where the Cr sites are in +2 oxidation state and are surrounded by 2 oxygen ligands; and ii) a Cr_2O_3-like phase, where the chromium sites belong to small CrO_6 octahedra partially aggregated, although not yet organized as for Cr_2O_3.

PERFORMANCES OF CR(II)-DHS SAMPLE IN ETHYLENE POLYMERIZATION

In a second moment, the performances of the CO-reduced Cr-DHS catalysts in ethylene polymerization were also tested. To this aim, the CO-reduced 0.5Cr-DHS catalyst was contacted with ethylene gas (P_{C2H4} = 500 mbar) at room temperature. A rapid decrease of the ethylene pressure was observed without any induction period, testifying that ethylene polymerization occurs. The catalyst was measured after ethylene polymerization.

XANES DATA

Figure 19 shows the XANES spectra of the 0.5Cr-DHS catalyst oxidized (black), CO-reduced (blue), and of the CO-reduced sample after ethylene polymerization at room temperature (P_{C2H4} = 500 mbar, pink). The first two spectra were discussed in the previous sections; the latter is completely different. This observation suggests that most of the chromium sites were involved in ethylene polymerization at room temperature, contrarily to what previously found by some of us for a Cr/SiO_2-aerosil sample in similar conditions.

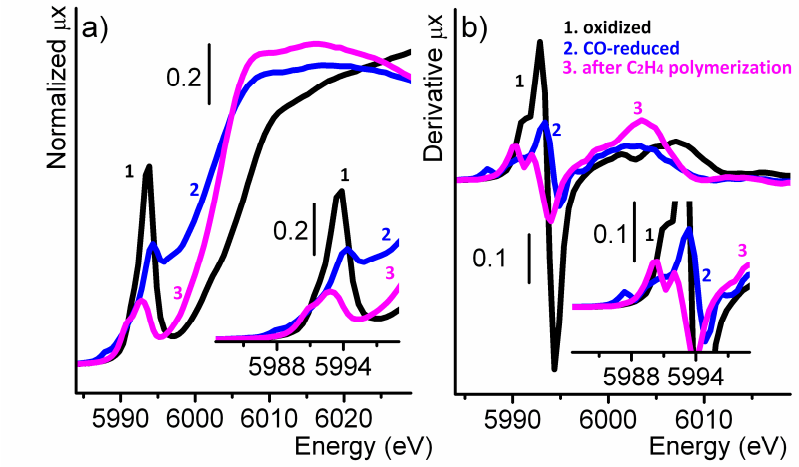

Figure 19 – Normalized XANES spectra (part a) and corresponding derivative signals (part b) of the 0.5Cr-DHS catalyst oxidized (black), CO-reduced (blue), and of the CO-reduced sample after ethylene polymerization at room temperature (P_{C2H4} = 500 mbar). The two insets show a magnification of the pre-edge region.

The pre-edge region is characterized by a double peak at 5991.0 – 5992.8 eV having a medium intensity. This double peak is at lower energy than that characteristic of the oxidized sample, and about one third less intense. It has been shown that the pre-edge region contains information on the coordination geometry of the chromium sites.[10-12] In particular, the presence of an intense pre-edge line, assigned to electron transition from Cr(1s) to molecular orbitals having mainly *d* character,[10] is indicative of a pseudo-tetrahedral coordination; the same transition is dipole-forbidden for coordination geometries that possess an inversion centre (such as octahedral). On these basis, the intensity of the pre-edge double peak observed in the spectrum of the catalyst after ethylene polymerization is in favour of chromium ions having a distorted tetrahedral geometry.

Coming to the energy position of the absorption threshold, in principle it should give a rough indication on the oxidation state of the Cr ion,[12-15] although it has been demonstrated

that many factors, such as the coordination geometry and the type of the ligands, can influence the edge position.[16] For the Cr-DHS catalyst after ethylene polymerization, the edge value (6003.5 eV) is intermediate with respect to those of the same sample oxidized (where all the Cr sites are in the +6 oxidation state) and CO-reduced (where all the Cr sites are in the +2 oxidation state). Hence, an intermediate oxidation state (either +4 or +3) could be hypothesized, assuming that the chromium species after ethylene polymerization do have a coordination geometry similar to that of the oxidized and CO-reduced species (low coordination) and similar ligands (such as oxygen and carbon).

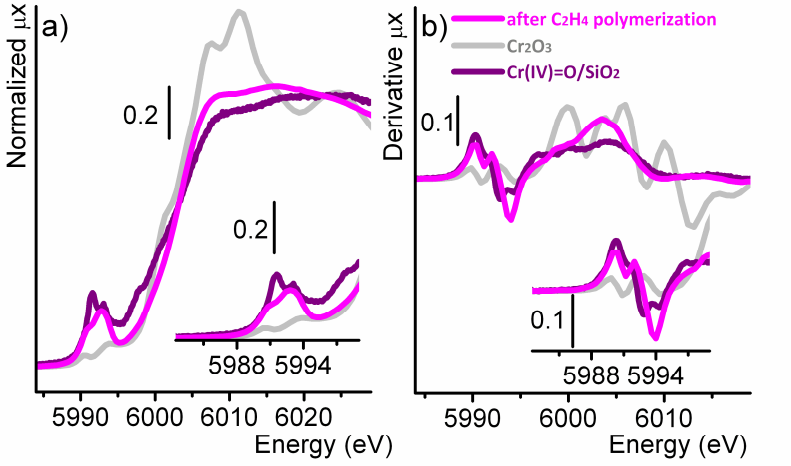

Figure 20 – Normalized XANES spectra (part a) and corresponding derivative signals (part b) of the CO-reduced 0.5Cr-DHS catalyst after ethylene polymerization at room temperature (P_{C2H4} = 500 mbar) compared to the XANES spectra of Cr_2O_3 (gray); and of a Cr(IV)=O/SiO_2 sample. The two insets show a magnification of the pre-edge region.

The oxidation state of the chromium sites active in ethylene polymerization is still a matter of debate in the specialized literature and, as a consequence, also the mechanism of initiation of the polymerization reaction is still unclear. In this respect, it should be noticed that the spectrum of the Cr-DHS catalyst after ethylene polymerization has a threshold edge very similar to that of the Cr_2O_3 reference compound (where chromium is in the +3 oxidation state), as shown in Figure 20 (compare pink and grey curves). This observation could suggest that the average oxidation state of the active Cr sites is +3. However, it should be noticed also that the coordination geometry of the chromium sites in our sample and in Cr_2O_3 is different (as suggested by the pre-edge region); hence, any comparison should be done with caution, as further demonstrated by the observation that in the white-line region the spectrum of the sample after ethylene polymerization is completely different from that of Cr_2O_3. Indeed, the XANES spectrum of the Cr-DHS catalyst after ethylene polymerization is also very similar to that of an analogous Cr/SiO_2-aerosil sample treated in N_2O (Figure 20, purple curve), where the chromium sites have been demonstrated to be in the +4 oxidation state, in the form of chromyl (mono-oxo species).[17] The two spectra are very similar not only in the edge region, but especially in the pre-edge one, where both of them are characterized by a double peak in the same energy region. This comparison suggests that the chromium sites active in ethylene polymerization do have a +4 oxidation state and a distorted tetrahedral geometry, similar to that characteristic of a silica-supported chromyl species.

Finally, it should be considered the possibility that the observed XANES spectrum results from the combination of the spectra of a fraction of un-reacted Cr(II) sites and a fraction of active Cr sites (more oxidized). In absence of a reference for the active chromium sites it is very difficult to estimate the fraction of active sites. Nevertheless, it should be noticed that the XANES spectrum of the CO-reduced Cr-DHS sample is characterized by a sharp feature at 5994.2 eV, where the spectrum of the same sample after ethylene polymerization does have a minimum. For this reason (and from the observation of the rapid decrease of ethylene pressure during the reaction), we conclude that the majority of the chromium sites in Cr-DHS catalyst are active in ethylene polymerization at room temperature. This is not trivial, since in the Phillips catalyst only a fraction of the total chromium sites are considered active in ethylene polymerization.[7, 18] The reasons for the higher activity of Cr-DHS catalyst might reside in the different silica support.

In conclusion, the XANES spectra shown in Figure 19 provide evidence that: i) the majority of the Cr(II) sites in Cr-DHS are active in ethylene polymerization at room temperature; ii) the active chromium sites are characterized by a distorted tetrahedral geometry and iii) have an oxidation state intermediate between +2 and +6. Although a discrimination between +3 and +4 is difficult, comparison with the spectrum of a silica-supported mono-oxo chromyl species suggests that +4 could be the average oxidation state.

QUALITATIVE ANALYSIS OF THE ROUGH EXAFS DATA

The k^3-weighted χ(k) function of the 0.5Cr-DHS catalyst after ethylene polymerization at room temperature is compared to those of the same sample oxidized and CO-reduced in Figure 21.

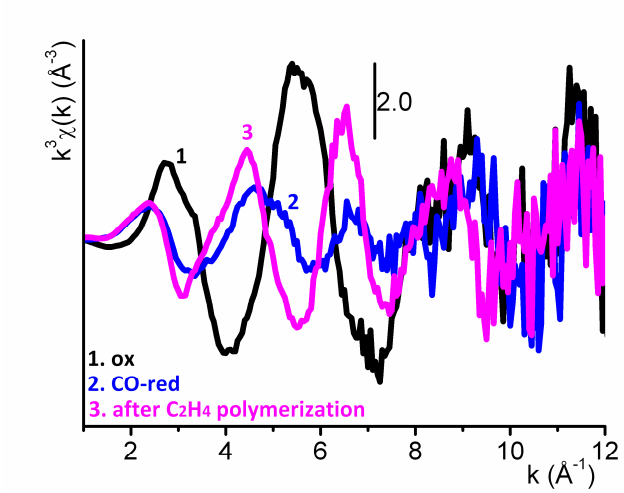

Figure 21 – k^3-weighted χ(k) functions of the 0.5Cr-DHS catalyst oxidized (black), CO-reduced (blue), and of the CO-reduced sample after ethylene polymerization at room temperature (P_{C2H4} = 500 mbar).

It is evident that the EXAFS signal is completely different from that of the CO-reduced parent material, testifying that the majority of the chromium sites have been involved in ethylene polymerization, as already determined by XANES spectra. Moreover, the EXAFS oscillations are more intense than for the CO-reduced sample, suggesting that the chromium sites are more homogenous from a structural point of view, as well as no destructive interference occurs between several scattering paths contributing in the same R region.

Figure 22 shows the Fourier Transforms in both modulus (part a) and imaginary parts (part b) of the k^3-weighted χ(k) functions (FT in the Δk = 1.0 – 11.0 $Å^{-1}$ range) for the CO-reduced 0.5Cr-DHS catalyst and for the same sample after ethylene polymerization at room temperature. In the spectrum of the sample after ethylene polymerization the first shell signal is much more intense and shifted towards longer distance than for the CO-reduced sample. The higher intensity could be explained in terms of a greater coordination number (as expected because of the presence of the polymer chains), but also because of the absence of the destructive interference between different Cr-O scattering paths, which characterize the signal of he CO-reduced sample (which can be due to a "ligand displacement" phenomenon induced by the presence of the polymer chains).

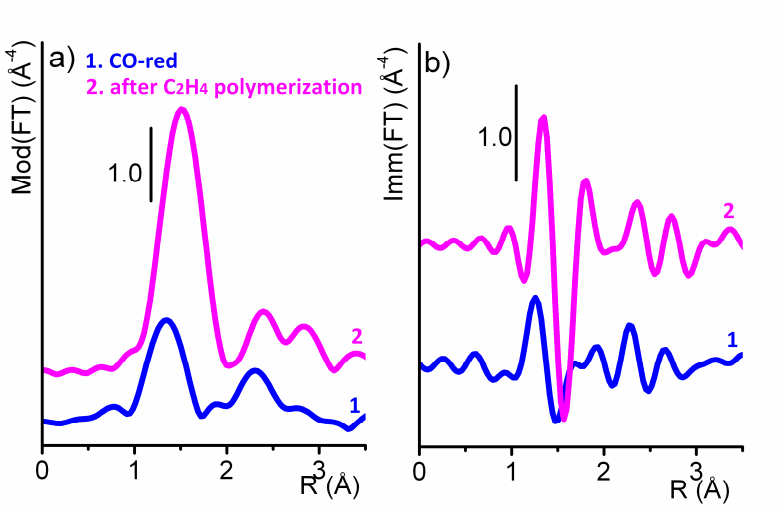

Figure 22 – Fourier Transforms in both modulus (part a) and imaginary parts (part b) of the k^3-weighted χ(k) functions (FT in the Δk = 1.0 – 11.0 $Å^{-1}$ range) of the 0.5Cr-DHS catalyst oxidized (black), CO-reduced (blue), and of the CO-reduced sample after ethylene polymerization at room temperature (P_{C2H4} = 500 mbar).

APPENDIX
THE LOCAL STRUCTURE OF Cr_2O_3 REFERENCE COMPOUND

Figure 23 shows the FT in both modulus (part a) and imaginary parts (part b) of the k^3-weighted χ(k) functions (FT in the Δk = 1.0 – 13 $Å^{-1}$ range). The experimental spectrum (dotted) is characterized by three main peaks centered at 1.5, 2.5, and 3.3 Å, respectively (not corrected in phase). The main scattering paths contributing to the EXAFS signal in the ΔR = 0.0 – 4.0 Å range are summarized in Table 12.

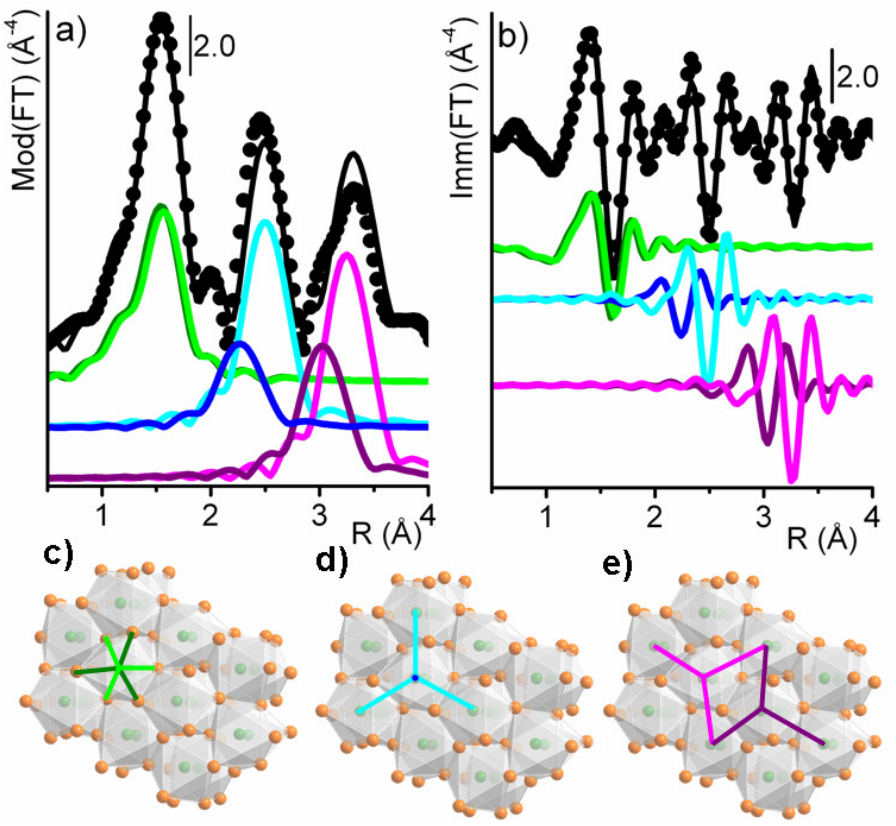

Figure 23 – Fourier Transforms in both modulus (part a) and imaginary parts (part b) of the k^3-weighted χ(k) functions (FT in the Δk = 1.0 – 13 $Å^{-1}$ range) of Cr_2O_3. The experimental spectrum (dotted) is compared to the best fit (full line) performed by considering the scattering paths shown in color and schematically represented in parts c) (oxygen ligands belonging to the first coordination sphere), part d) (chromium ligands belonging to the second coordination sphere), and e) (chromium ligands belonging to the third coordination sphere).

The first shell peak is due to the contribution of 6 oxygen ligands at almost the same distance (green curves). The main contributions to the second peak come from 3 chromium ligands at 2.626 Å (cyan curves), whereas a fourth chromium at 2.862 Å (blue curve) is the responsible of the beat at around 2.07 Å well evident in the imaginary part. Finally, the third peak is mainly due to the contribution of 3 chromium ligands at 3.617Å (pink curve); also in this case, the presence of additional 3 chromium ligands at 3.394 Å (violet curve) causes a beat at 2.9 Å in the Imm(FT).

Table 12 – List the main scattering paths contributing to the EXAFS spectrum of Cr_2O_3 in the ΔR = 1.0 – 4.0 Å range. For each path, the type of ligands ([+] is the absorbing Cr atom), the degeneracy and the length (as determined by XRD data) are indicated.

Shell	Scattering Path	Deg.	Length (Å)
1st shell	[+] O [+]	3	1.956
	[+] O [+]	3	1.981
2nd shell	[+] Cr [+]	3	2.626
	[+] Cr [+]	1	2.862
3rd shell	[+] Cr [+]	3	3.394
	[+] Cr [+]	3	3.617

The experimental spectrum was fitted by considering the contribution of these 6 single scattering (SS) paths only. The following fitting variables have been used:

i) a single ΔE_0 common to all the paths;
ii) a single S_0^2 common to all the paths;
iii) the isotropic coefficient α (the real distance R' being defined as $R' = R_{eff} * \alpha$);
iv) two different Debye-Waller factors for the paths involving oxygen and chromium ligands, respectively.

The best fit is shown in Figure 23 (full line), and a summary of the results is given in Table 13.

Table 13 – Optimized parameters in EXAFS analysis (performed in the ΔR = 1.0 – 4.0 Å range, FT in 1.0–13.0 A^{-1} k-range) for Cr_2O_3. The fit resulted in R_{factor}=0.049.

Variable	Fitting result
S^0_2	0.7 ± 0.1
ΔE_0	-3.2 ± 0.8 eV
α	1.014 ± 0.002
σ^2(O)	0.0034 ± 0.0008 $Å^2$
σ^2(Cr)	0.0040 ± 0.0007 $Å^2$

References

1. B. M. Weckhuysen, R. A. Schoonheydt, J. M. Jehng, I. E. Wachs, S. J. Cho, R. Ryoo, S. Kijlstra and E. Poels, *J. Chem. Soc. Faraday Trans.*, 1995, **91**, 3245-3253.
2. B. M. Weckhuysen, A. A. Verberckmoes, A. R. DeBaets and R. A. Schoonheydt, *J. Catal.*, 1997, **166**, 160-171.
3. C. Pak and G. L. Haller, *Micropor. Mesopor. Mat.*, 2001, **48**, 165-170.
4. Y. Wang, Y. Ohishi, T. Shishido, Q. H. Zhang, W. Yang, Q. Guo, H. L. Wan and K. Takehira, *J. Catal.*, 2003, **220**, 347-357.
5. E. Groppo, C. Prestipino, F. Cesano, F. Bonino, S. Bordiga, C. Lamberti, P. C. Thüne, J. W. Niemantsverdriet and A. Zecchina, *J. Catal.*, 2005, **230**, 98-108.
6. S. Bordiga, E. Groppo, G. Agostini, J. A. Van Bokhoven and C. Lamberti, *Chem. Rev.*, 2013, **113**, dx.doi.org/10.1021/cr2000898.
7. E. Groppo, C. Lamberti, S. Bordiga, G. Spoto and A. Zecchina, *Chem. Rev.*, 2005, **105**, 115-183.
8. D. Gianolio, E. Groppo, J. G. Vitillo, A. Damin, S. Bordiga, A. Zecchina and C. Lamberti, *Chem. Commun.*, 2010, **46**, 976–978.
9. X. Wang, X. Ma, S. Zhao, B. Wang and C. Song, *Energy Environ. Sci.*, 2009, **2**, 878 - 882.
10. J. Wong, F. W. Lytle, R. P. Messmer and D. H. Maylotte, *Phys. Rev. B*, 1984, **30**, 5595.
11. L. Garcia, M. Benfatto, C. R. Natoli, A. Bianconi, I. Davoli and A. Marcelli, *Solid. State Commun.*, 1986, **58**, 595.
12. A. Pantelouris, H. Modrovw, M. Pantelouris, J. Hormes and D. Reinen, *Chem. Phys.*, 2004, **300**, 13-22.
13. C. Jousseaume, F. Ribot, A. Kahn-Harari, D. Vivien and F. Villain, *Nucl. Instrum. Meth. B*, 2003, **200**, 425-431.
14. C. Jousseaume, D. Vivien, A. Kahn-Harari, J. Derouet, F. Ribot and F. Villain, *J. Appl. Phys.*, 2003, **93**, 6006-6015.
15. I. Arcon, B. Mirtic and A. Kodre, *J. Am. Chem. Soc.*, 1998, **81**, 222-224.
16. M. Tromp, J. O. Moulin, G. Reid and J. Evans, *AIP Conf. Proc.*, 2007, **882**, 699-701.
17. E. Groppo, A. Damin, C. Otero Arean and A. Zecchina, *Chem. Eur. J.*, 2011, **17**, 11110 – 11114.
18. E. Groppo, C. Lamberti, F. Cesano and A. Zecchina, *Phys. Chem. Chem. Phys.*, 2006, **8**, 2453-2456.